EPJ Nuclear Sci. Technol. **10**, 13 (2024)

https://doi.org/10.1051/epjn/2024012

EPJ Nuclear Sciences & Technologies

Available online at:
https://www.epj-n.org

Status and advances of Monte Carlo codes for particle transport simulation, edited by Andrea Zoia, Cheikh Diop and Cyrille de Saint Jean

REGULAR ARTICLE

OPEN ACCESS

Overview of PHITS Ver.3.34 with particular focus on track-structure calculation

Tatsuhiko Ogawa[1,*], Yuho Hirata[1], Yusuke Matsuya[1,2], Takeshi Kai[1], Tatsuhiko Sato[1], Yosuke Iwamoto[1], Shintaro Hashimoto[1], Takuya Furuta[1], Shin-ichiro Abe[1], Norihiro Matsuda[1], Takuya Sekikawa[1], Lan Yao[1], Pi-En Tsai[1,3], Hunter N. Ratliff[4], Hiroshi Iwase[5], Yasuhito Sakaki[5], Kenta Sugihara[5], Nobuhiro Shigyo[6], Lembit Sihver[7], and Koji Niita[8]

[1] Japan Atomic Energy Agency, Shirakata 2-4, Tokai, Ibaraki, Japan
[2] Hokkaido University, Faculty of Health Sciences, N-12-W-5, Kita-ku, Sapporo, Hokkaido, Japan
[3] Current affiliation: Zap energy, Everett, Washington, USA
[4] Western Norway University of Applied Sciences, Høgskulen på Vestlandet, Postbox 7030, 5020 Bergen, Norway
[5] Radiation Science Center, High Energy Accelerator Research Organization, Ibaraki, Japan
[6] Kyushu University, Department of Applied Quantum Physics and Nuclear Engineering, Fukuoka, Japan
[7] Department of Radiation Physics, Technische Universität Wien, Atominstitut, Vienna, Austria
[8] Research Organization for Information Science and Technology, Shirakata 2-4, Tokai, Ibaraki, Japan

Received: 11 June 2024 / Received in final form: 25 July 2024 / Accepted: 27 August 2024

Abstract. This paper presents the latest updates on PHITS, a versatile radiation transport code, focusing specifically on track-structure models. Track structure calculations are methods used to simulate the movement of charged particles while explicitly considering each atomic reaction. Initially developed for radiation biology, these calculation methods aimed to analyze the radiation-induced damage to DNA and chromosomes. Several track-structure calculation models, including PHITS-ETS, PHITS-ETS for Si, PHITS-KURBUC, ETSART, and ITSART, have been developed and implemented for PHITS. These models allow users to study the behavior of various particles at the nano-scale across a wide range of materials. Furthermore, potential applications of track-structure calculations have also been proposed so far. This collection of track-structure calculation models, which encompasses diverse conditions, opens up new avenues for research in the field of radiation effects.

1 Introduction

Particle and Heavy Ion Transport code System, PHITS [1,2] is a general-purpose radiation transport code, originally developed for the design of J-PARC (Japan Proton Accelerator Research Complex), and is used world-wide in various fields. Due to its role in the design of J-PARC, the transport of protons and ions, simulated by ATIMA (ATomic Interaction with MAtter) [3–5] and that of electrons and positrons by EGS5 (Electron Gamma Shower Ver.5) [6], are the most accurate parts of PHITS.

PHITS Ver.3.33, mostly equivalent to Ver.3.34, is detailed elsewhere [2]; therefore, this paper will primarily discuss the recent advancements in the development and applications of track-structure models. The Track-Structure Model (TSM) is a method of charged particle transport that simulates the paths of charged particles as a series of discrete atomic reactions. Due to the highly frequent interactions of charged particles in matter, their transport is usually simulated by either the condensed-history method (CHM) or the continuous slowing-down approximation, both of which represent particle flight steps as the summation of roughly 1000 to 1 000 000 atomic reactions. TSM, on the other hand, offers the capability to simulate charged particle transport with an atomic-scale spatial resolution at the price of computational time. Numerous models for TSM have been developed, primarily to study the biological effects of radiation exposure [7–19].

In light of this, PHITS-ETS[20] and PHITS-KURBUC [21] for accurate microdosimetry in liquid water and "PHITS-ETS for Si" [22] for Si were developed and implemented in PHITS. Furthermore, TSMs that can be applied to a broader range of materials, such as ETSART (Electron Track Structure mode applicable to ARbitrary Targets) [23] and ITSART (Ion Track Structure mode applicable to ARbitrary Targets) [24], have also been developed and added to PHITS.

Among a variety of general-purpose Monte-Carlo radiation transport codes [25–31], Geant4 includes a TSM

* e-mail: ogawa.tatsuhiko@jaea.go.jp

Table 1. Track-structure calculation models available in PHITS Ver.3.34.

	Medium	Particle	Minimum energy	Maximum energy
PHITS-ETS	Liquid water	Electrons, positrons	1 meV	1 TeV
PHITS-ETS for Si	Si	Electrons, positrons	1 eV	100 keV
PHITS-KURBUC	Liquid water	Protons	1 keV	300 MeV
		Carbon ions	1 keV/n	10 MeV/n
ETSART	Semiconductors	Electrons, positrons	1 eV	1 TeV
ITSART	Arbitrary materials	Protons (and ions)	1 eV	1 TeV

for liquid water, known as Geant4-DNA, which is comparable to PHITS-ETS and PHITS-KURBUC. Meanwhile, PHITS is advantageous thanks to its unique TSMs which are applicable to arbitrary materials.

This paper presents the current state of TSM development in PHITS as well as its advanced applications, such as microdosimetric quantity calculation, DNA damage modeling, radical production simulation, prediction of luminescent yields, and calculation of displacement per atom (DPA).

2 Features of PHITS Ver.3.34

From Ver.3.02 to Ver.3.34, PHITS was upgraded as described below. More details are described in the original article [2].

- Reaction and transport models
  - Implementation of the interface to read ACE-format cross-section data libraries for deuterons, alphas, and photons[1].
  - Bundling an essential part of the JENDL-5 cross-section data library [32], including the isotopic abundance configuration for all JENDL library files.
  - Implementation of the interface to read user-defined stopping power.
  - Implementation of neutrino reaction models.
  - Upgrade of the fission model for sub-actinides [33].
  - Upgrade of the gamma de-excitation model EBITEM [34].
  - Implementation of photon-induced muon pair production model [35].
  - Implementation of continuous-energy photon adjoint calculation function [36].
  - Implementation of an interface to handle particles, cross-sections, reactions, and decays defined by users.
  - Implementation of a function to invoke cosmic ray sources [37–43].
  - Implementation of TSM discussed in this paper.
- Tallies
  - Implementation of *anatally*, a function to perform numerical analyses of more than one tally.
  - Upgrade of DPA calculation tally "[T-DPA]" to use arc-DPA model [44] for a higher accuracy [45].
  - Upgrade of microdosimetric quantity tally "[T-SED]" [46].
- Pre/Post-processes
  - Implementation of an interface to read NASTRAN bulk data and write OpenFOAM field data to be coupled with thermo-fluid simulation software.
  - Implementation of an interface to read electromagnetic field data written in XYZ or R-Z coordinate format.
  - Upgrade of the burn-up calculation post-processor DCHAIN-PHITS [47] formerly referred to as DCHAIN-SP.
  - Implementation of the organic scintillator response function simulator SCINFUL-QMD [48,49]. High-precision cross-section data used in SCINFUL-QMD was implemented accordingly.

[1] Photon cross-section data means photo-nuclear reaction cross section data. Atomic reactions are handled by EGS5 [6]. The interface for protons, and neutrons above 20 MeV, was implemented before Ver. 3.02.

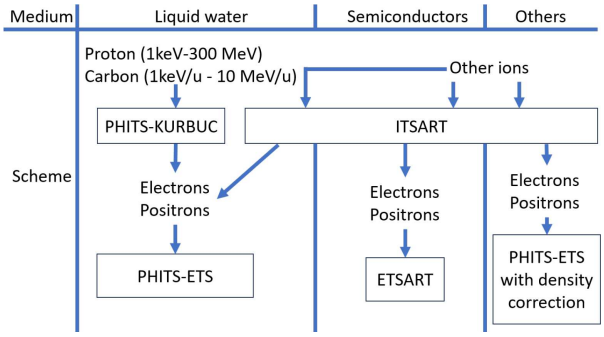

Fig. 1. Track-structure calculation scheme in the recommended configuration.

Among all of the above updates, the development of TSMs was one of the highlights. Table 1 shows a list of TSMs implemented in the latest version of PHITS. They cover different particles, transport media, and energy ranges, to cover a wide variety of conditions. Figure 1 depicts how these models are connected. More detail on each TSM model is described below.

2.1 High-precision TSM for specific materials

PHITS-ETS, "PHITS-ETS for Si" and PHITS-KURBUC are high-precision TSMs in PHITS. They are capable of performing detailed calculations on a limited range of

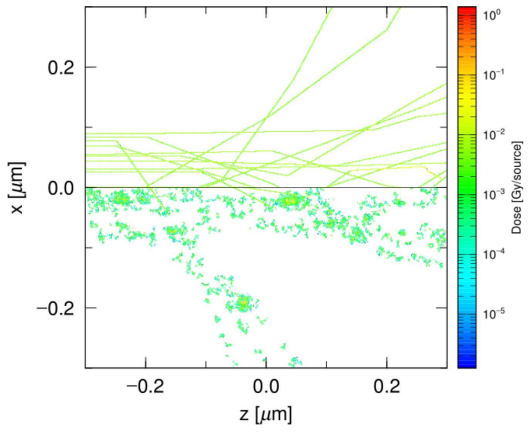

Fig. 2. Energy deposition by electrons with initial kinetic energy 10 keV injected in liquid water from the left. PHITS-ETS is used in $x \leq 0$ while conventional model EGS5 is used in $x \geq 0$.

particle species, accurately identifying atomic reaction channels in liquid water and solid silicon. PHITS-ETS was integrated prior to PHITS Ver.3.02, but it is briefly reviewed here due to its importance to other TSMs downstream.

The predecessor to PHITS-ETS was a standalone code DMCC (Dynamic Monte Carlo Code, DMCC) [20] intended to track the transport of electrons in liquid water, taking into account the atomic-scale mechanisms responsible for electron deceleration, down to 1 meV. Besides the dominant reaction channels above 7 eV, such as ionizations and electronic excitations, PHITS-ETS also considers dissociative electron attachment, stretching, bending, and rotational excitation modes of water molecules, as well as translational and liberational phonons. DMCC simulated the attractive force of cations on electrons [50], especially important for electrons below 1 eV. However, to integrate it into PHITS, the features that were incompatible with PHITS's assumption of a time-independent medium were removed. Electrons that were down-scattered to the switching energy from the EGS mode to the TSM were directed towards the PHITS-ETS algorithm. The stopping range and power of electrons incorporated into PHITS-ETS [51,52] were benchmarked and used to predict DNA strand breaks. PHITS-ETS is applicable for electrons and positrons above 1 eV in liquid water. Figure 2 illustrates the energy deposition in liquid water exposed to 20 electrons of 10 keV, as calculated by PHITS-ETS and EGS5 in the lower and upper halves, respectively. In the y direction, the events from – 1 mm to +1 mm are shown. The electron tracks calculated by EGS5 are depicted as straight lines connected by bends that represent scatterings, with energy deposition treated as an event spread over the flight path. In contrast, energy deposition calculated by PHITS-ETS is represented as dots corresponding to discrete events. Regardless of the starting point, the models used for particles crossing $x = 0$ border are switched from/to TSM.

"PHITS-ETS for Si" was developed within PHITS to perform highly precise track-structure calculations in silicon [22]. Unlike PHITS-ETS, which was initially developed separately from PHITS, this code was created as an integral part of PHITS. Contrary to water, whose atomic reaction cross sections have been measured in various experiments (e.g. [53]), creating solid silicon targets small enough for a single atomic reaction to be observable is not feasible. Hence, "PHITS-ETS for Si" begins with the Optical Energy Loss Function (OELF), which characterizes the interaction of silicon atoms and photons and has been measured as optical responses. Given that the interaction between the projectile electrons and target atoms is mediated by virtual photons, the OELF can be converted into the Electron Energy Loss Function (EELF) [54]. This can be further converted into a Single-Differential electron scattering Cross Section (SDCS) via the Drude formalism. To identify atomic interaction channels, such as ionization, phonon excitation, and electronic excitation, the OELF was broken down into reaction channels before being converted to EELF. The partial OELF corresponding to each reaction channel was independently converted to SDCS and summed up for transport calculation. "PHITS-ETS for Si" samples the reaction modes at a probability proportional to the partial cross-section corresponding to the mode. "PHITS-ETS for Si" can be used for electrons from 1 eV to 100 keV in silicon, where the dielectric function in the corresponding frequency range was evaluated. Its stopping power, electron path lengths, and energy deposition depth profiles are benchmarked against experimental data. A notable difference between PHITS-ETS and "PHITS-ETS for Si" is the transport of excited electrons. In PHITS-ETS, excited electrons are localized due to the insulating nature of liquid water, unless they are knocked out to the vacuum level. However, in "PHITS-ETS for Si", excited electrons can travel further by both ionization and excitation, as electrons beyond the band-gap can travel in the conduction band. Shown in Figure 3 is the energy deposition in Si exposed to 20 electrons of 2 keV calculated using "PHITS-ETS for Si" and EGS in the lower half and the upper half, respectively. Similarly, with Figure 2, the energy deposition calculated by EGS5 is spread over the flight paths, and the energy deposition calculated by "PHITS-ETS for Si" is shown as dots representing discrete events. In contrast to Figure 2, the lower half of Figure 3 illustrates that the reaction-free path is much shorter due to the larger electron density of Si.

PHITS-KURBUC is another TSM of PHITS dedicated to the transport of protons and carbon ions in liquid water. This model is based on KURBUC (Kyushu University and Radio-biology Unit Code) developed by Nikjoo et al. [11,55] irrespective of PHITS. KURBUC, intended for proton therapy and carbon ion therapy, has exclusive cross sections of single target ionization, double target ionization, loss ionization, single projectile electron loss, single electron capture, transfer ionization, target excitation, and nuclear elastic scattering, to transport the projectiles with identification of reaction channels. The projectile charge state changed through the ionization or charge transfer reactions is identified at every transport step. PHITS-KURBUC, one of the versions of KURBUC, was branched from its official standalone version and

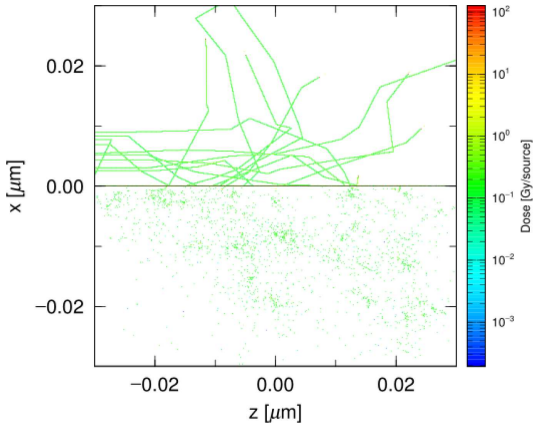

Fig. 3. Energy deposition by electrons with initial kinetic energy 2 keV injected in Si from the left. "PHITS-ETS for Si" is used in $x \leq 0$ while conventional model EGS5 is used in $x \geq 0$.

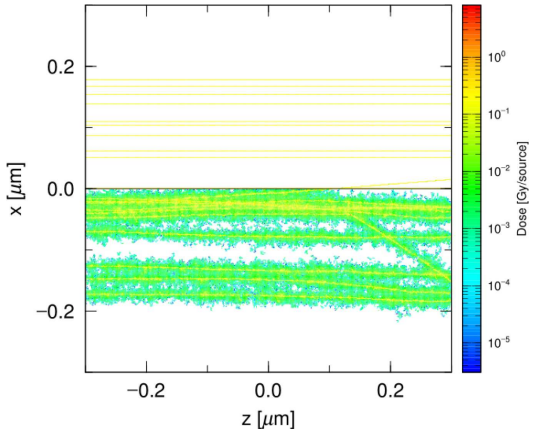

Fig. 4. Energy deposition by protons with an initial kinetic energy of 200 keV injected into liquid water from the left. PHITS-KURBUC is used in $x \leq 0$ while conventional transport model based on ATIMA is used in $x \geq 0$.

incorporated into PHITS. Benchmarking of its cross sections, particle stopping ranges, radial dose distribution, and lineal energy distribution against experimental data, other codes, and the original KURBUC confirm its accuracy [21]. PHITS-KURBUC can be used for protons below 300 MeV and carbon ions below 10 MeV/n in liquid water. In the energy range above these upper limits, users can choose continuous slowing down calculation by ATIMA or the generalized track structure model ITSART, which is described later. Electrons produced in PHITS-KURBUC are passed to PHITS-ETS to be tracked down to thermalization, achieving a high-precision track structure simulation scheme. Shown in Figure 4 is the energy deposition in liquid water exposed to 20 protons of 200 keV calculated using PHITS-KURBUC and ATIMA in the lower half and the upper half, respectively. Unlike electrons, protons densely generate secondary electrons as illustrated in the lower half. In contrast, the energy deposition attributed to ionization is treated as continuous slowing down represented as straight lines in the upper half.

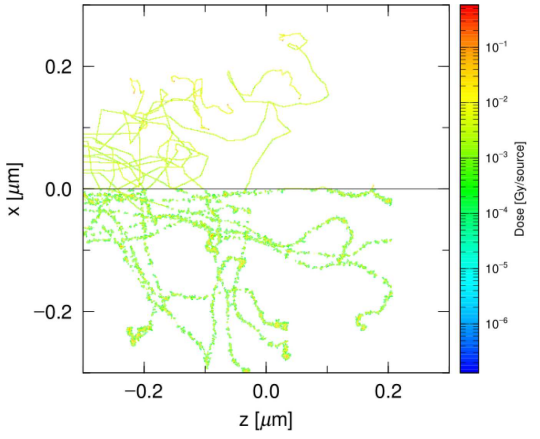

Fig. 5. Energy deposition by protons with an initial kinetic energy 10 keV injected to GaAs from the left. ETSART is used in $x \leq 0$ while conventional transport model based on EGS is used in $x \geq 0$.

2.2 Generalized TSM

In contrast to the high-precision TSMs described earlier, PHITS includes another series of TSMs that can be applied to a wide variety of materials. ETSART is one of these models, suitable for electrons and positrons in arbitrary semiconductor materials. ITSART is another generalized TSM, applicable to protons in any medium. The application of these models is not limited to a single material like the high-precision models, but this comes at the expense of cross-section accuracy or the exclusive identification of reaction channels.

ETSART is based on the total and singly differential cross sections calculated by the binary-encounter-Bethe formula [56–58] and the characteristic energies of the matter, namely orbital electron binding energies, orbital electron kinetic energies, and plasmon energies. Apart from these element-specific energies (which are taken from the default data library sets of PHITS), users are required to provide the band gap energy to ETSART as one of the input parameters. ETSART was validated by comparing the projected range in liquid water calculated by ETSART with that taken from the ICRU report 37 [59]. To demonstrate its capability to simulate various materials, ETSART was used to calculate the average energy of electron-hole pair generation (often referred to as ϵ) for 14 semiconductor materials. The results agreed well with the measured ϵ of the earlier experiments [23]. Shown in Figure 5 is the energy deposition in GaAs exposed to 20 electrons of 10 keV calculated using ETSART and EGS in the lower half and the upper half, respectively. Due to the large electron density of GaAs compared with Figures 2 and 3, electron trajectories are deflected in both upper and lower halves. In the lower half, energy deposition simulated by ETSART is described as small points.

ITSART uses Rudd's formula [60] to calculate the single-differential cross section (SDCS) of each electron

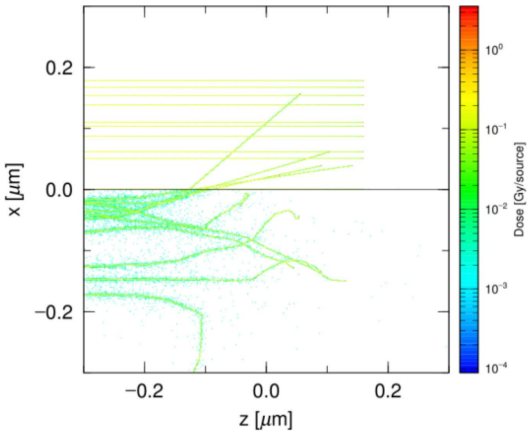

Fig. 6. Energy deposition by Li with an initial kinetic energy 20 keV/n injected to Fe from the left. ITSART and ETSART are used in $x \leq 0$ while conventional transport model based on ATIMA and EGS is used in $x \geq 0$.

orbit in the target matter. By integrating this SDCS, weighted by the outgoing kinetic energy and the binding energy of the ejected electron, the partial linear energy transfer (LET) attributable to ionization is obtained. The kinetic energy of the projectile is reduced by the total LET calculated by ATIMA, from which the partial LET is subtracted. ITSART does not consider other channels such as charge exchange reactions, excitation reactions, and Rutherford scattering, but the total stopping power is conserved by the above method, called restricted energy loss calculation. Because both ATIMA and Rudd's formula are apply arbitrary materials, ITSART does not have any restrictions on the target materials. After the first version was published in 2021 [24], the latest versions [61] can simulate Rutherford scattering and injection of ions. ITSART reads the chemical form of the target material specified by the users and adjusts the parameters of Rudd's formula based on the table given by Rudd [62]. As illustrated in Figure 1, protons and carbon ions with energy outside the coverage of KURBUC are handled by ITSART. For example, protons of 400 MeV are transported by ITSART down to 300 MeV and then passed to KURBUC. This allows users to perform a full track-structure calculation of therapeutic charged particle beams. Shown in Figure 6 is the energy deposition in Fe exposed to 20 ^{7}Li ions with an initial kinetic energy of 20 keV/n calculated using ITSART and ATIMA in the lower half and the upper half, respectively. In the lower half, ionization reactions by secondary electrons are seen as the haze around the trajectories of projectile. Despite the different calculation algorithms, the stopping ranges are consistent. ITSART can thus perform track structure calculations of arbitrary ions in arbitrary materials, with the produced electrons transported by ETSART.

2.3 Applications of TSMs

PHITS team suggests new applications and provides the tools necessary for such implementations.

TSMs are powerful tools for examining the spatial and probabilistic distributions of energy deposition by radiation, but the details of every single reaction are not always necessary. For instance, when the amount of energy deposited in an array of cells is of interest, the exact spatial coordinates of the energy deposition inside the cells are not crucial. The frequency distribution, as a function of the energy deposited in cells, can be useful data for explaining cell survival [63–67], and luminescence efficiency [68–70], assuming that the cells are biological cells or effective unit volume of phosphors. The [T-SED] tally function in PHITS, which calculates such microdosimetric distributions [71,72], was updated based on systematic trends of microdosimetric distributions reevaluated using the latest TSMs [46].

The DNA damage model is a tool [51,73,74] designed to estimate DNA single-strand break (SSB), double-strand break (DSB), and complex DSB (a DSB and another strand break adjacent within 10 base-pair distance) caused by electrons and protons. This model uses the spatial coordinates of ionization and excitation reactions calculated by PHITS-ETS and PHITS-KURBUC to estimate the yields of SSD, DSB, and complex DSB, the types of which are sensitive to the distance between the strands broken by atomic reactions. The SSB and DSB yields calculated by this model, in combination with PHITS-ETS and PHITS-KURBUC, are in good agreement with experimental data [73,75] of electrons and protons.

In addition to the direct hits considered by the above tool, DNAs are damaged by oxidation due to radical species produced by radiation. To account for such indirect damages, a post-process code called PHITS-Chem [76] was developed for the prediction of the time evolution of radical species ($\bullet$OH, e^{-}_{aq}, H_2, H_2O_2, etc.) produced by electrons and radical scavengers in liquid water. The reaction channels identified in PHITS-ETS are passed along with their spatial coordinates to calculate further spatial and temporal evolution resulting in radical species. Using branching ratios from atomic reaction to radical species, diffusion constants of radical species, reaction rate constants, and reaction radii of 35 chemical reactions between radical species pairs are calculated by solving finite difference equations with a time step of 1 ps. The dependence of radical yield on time and primary electron energies was benchmarked against the available experimental data. PHITS-Chem will be further improved to handle the above procedure for heavy ion incidence.

The responses of radiation detectors are usually assumed to be proportional to the energy deposition, but experimental data suggest that this proportionality does not hold true in the case of high-LET radiation (e.g. [77]). Based on a hypothesis that detector responses are modulated due to saturation or annihilation of the element responsible for detector output (e.g. electron-hole pairs in semiconductors, color centers in phosphors), our studies proposed to use the spatial coordinates of electrons, ionization, and excitation calculated by track-structure calculations [23,68,70] to estimate detector responses. In semiconductors, detection signals are proportional to the number of carriers reaching the electrodes. When the carrier density is high, random annihilation of the

electron-hole pair is more likely. Annihilated carriers no longer contribute to detection signals. In the case of phosphors, deexcitation of electrons through the color center, the mechanism responsible for fluorescent light emission, bottlenecks at the finite color centers. When the color centers are saturated by dense excited electrons, some of the electrons are not allowed to deexcite through the color centers, which leads to quenching. The light yields of BaFBr:Eu phosphors exposed to ions [68] and the amount of electron-hole pairs in various semiconductors [23] were successfully predicted. The quenching effect in organic scintillators was explained by the Förster effect [70], by which an excited electron transfers its energy to another. The donor electrons are deexcited to the ground state, and the recipient electrons come back to the original excitation state by non-radiative energy loss. In either case, the nm-scale spatial arrangement of excited electrons, which are predicted by track-structure calculation, plays a crucial role given that the above-mentioned reaction mechanisms have nm-scale reaction radii.

Lastly, TSM can be used to predict atomic displacement, which is important for radiation damage [61]. The target nuclei recoiled either by Rutherford scattering, which can be simulated by ITSART, or by nuclear reactions were scored and sent to an off-line post-processing tool to consider atomic displacement cascade based on the Kinchin-Pease [78] model. The conventional DPA calculation function implemented in PHITS [45,79] is designed to calculate DPA quickly by disregarding the event-by-event kinetics of Rutherford scattering. In contrast, TSM can predict the spatial arrangement of atomic displacement on the scale of nanometers. This feature is intended to be coupled with further processes such as the formation of dislocation for which the collective arrangement of defects is the key. Another advantage of PHITS is the calculation of DPA by nuclear reactions. SRIM [80] is known as a reliable code for predicting DPA; however, DPA produced through nuclear reactions cannot be considered. By calculating the momentum of the recoiled target and secondary particles by the built-in nuclear reaction models [81–83], ITSART can even calculate DPA by neutrons and photons, which is one of the remarkable advantages of TSM in PHITS.

3 Summary and future outlook

PHITS Version 3.34 includes various functions that have been developed and implemented since the release of Version 3.02. Among these, the track-structure models (TSMs) are novel and unique features. In PHITS, the TSM suite is made up of material-specific high-precision models—PHITS-ETS, PHITS-KURBUC, and "PHITS-ETS for Si"—and generalized models, ETSART and ITSART. This combination enables accurate simulations necessary for liquid water and silicon, while also allowing users to perform track-structure calculations in other materials. Given that the effects of radiation ultimately stem from microscopic energy deposition, TSMs will be useful in studying irradiation effects in various materials, such as ceramics, metals, phosphors, polymers, semiconductors, and superconductors.

Given the above progress, the PHITS team has the following future development plans, One of the most significant improvements in high-precision models is their ability to cover non-polar solvents. In liquid water, the electrons knocked out from atoms are hydrated due to the polarization of water molecules. Hydrated electrons can no longer dissociate water molecules because they possess less energy than free electrons. However, electrons in non-polar solvents do not have equivalent states to hydration, so these free electrons can remain energetic enough to disintegrate the solvent molecules. This mechanism is important for understanding radiation damage in reprocessing solvents. Generalized models are being improved to cover a wider range of conditions and to achieve greater precision. Particularly, the ETSART model, currently applicable only to semiconductors and some insulators, is being expanded to cover metals. The expansion of ITSART to explicitly consider more atomic reactions such as charge-changing reactions is underway. Furthermore, for both types of generalized TSMs, the transportation of holes is one of the significant future steps. Electrons at the bottom of the conduction band recombine with holes, releasing band-gap energy. Currently, this behavior is simulated solely by the transport of electrons, but ideally, the presence of holes should also be considered.

Acknowledgments

The Author (T.O.) would like to thank Dr. Daiki Satoh of the Japan Atomic Energy Agency for providing the cluster computer calculation resource, which was used in this research.

Funding

This work was partly supported by JSPS KAKENHI Grant Number 23K04635.

Conflicts of interest

The authors declare that they have no competing interests to report.

Data availability statement

The data will be made available by the corresponding author on reasonable requests.

Author contribution statement

Tatsuhiko Ogawa, Yuho Hirata, Yusuke Matsuya, Takeshi Kai, Tatsuhiko Sato, and Takuya Sekikawa performed conceptualization, coding, and analysis concerning track structure models. Yosuke Iwamoto, Shintaro Hashimoto, Takuya Furuta, Shin-ichiro Abe, Norihiro Matsuda, Hunter N. Ratliff, Pi-En Tsai, Hiroshi Iwase, Yasuhito Sakaki, Kenta Sugihara, Nobuhiro Shigyo, and Koji Niita contributed through conceptualization, coding, and analysis of the parts other than track structure models listed at the beginning of Section 2. Lan Yao worked on data curation and project administration. Lembit Sihver reviewed the manuscript.

References

1. T. Sato, Y. Iwamoto, S. Hashimoto, T. Ogawa, T. Furuta, S. Abe, T. Kai, P.E. Tsai, N. Matsuda, H. Iwase et al., J. Nucl. Sci. Technol. **55**, 684 (2018)

2. T. Sato, Y. Iwamoto, S. Hashimoto, T. Ogawa, T. Furuta, S. Abe, T. Kai, Y. Matsuya, N. Matsuda, Y. Hirata et al., J. Nucl. Sci. Technol. **61**, 127 (2024)
3. https://web-docs.gsi.de/~weick/atima/ (2024)
4. H. Weick, H. Geissel, N. Iwasa, C. Scheidenberger, J.R. Sanchez, A. Prochazka, S. Purushotaman, GSI Scientific Report, pp. 2018–1 (2017)
5. H. Paul, Nucl. Instrum. Meth. Phys. Res. B: Beam Interactions with Materials and Atoms **268**, 3421 (2010)
6. H. Hirayama, Y. Namito, W.R. Nelson, A.F. Bielajew, S.J. Wilderman, U. Michigan, Tech. rep., United States (Department of Energy 2005)
7. S. Incerti, M. Douglass, S. Penfold, S. Guatelli, E. Bezak, Phys. Medica **32**, 1187 (2016)
8. I. Plante, F.A. Cucinotta, Monte-Carlo Simulation of Ionizing Radiation Tracks, Applications of Monte Carlo Methods in Biology, Medicine and Other Fields of Science, (2011)
9. M. Zaider, D.J. Brenner, W.E. Wilson, Radiat. Res. **95**, 231 (1983)
10. V. Conte, P. Colautti, B. Grosswendt, D. Moro, L.D. Nardo, New J. Phys. **14**, 093010 (2012)
11. H. Nikjoo, S. Uehara, D. Emfietzoglou, *Interaction of Radiation with Matter* (CRC Press, Boca Raton, 2012)
12. A. Ito, in *Nuclear and atomic data for radiotherapy and related radiobiology* (1987)
13. J. Fernández-Varea, D. Liljequist, S. Csillag, R. Räty, F. Salvat, Nucl. Instrum. Meth. Phys. Res. B: Beam Interactions with Materials and Atoms **108**, 35 (1996)
14. S. Uehara, H. Nikjoo, D.T. Goodhead, Phys. Med. Biol. **38**, 1841 (1993)
15. J. Turner, J. Magee, H. Wright, A. Chatterjee, R. Hamm, R. Ritchie, Radiat. Res. **96**, 437 (1983)
16. W. Friedland, P. Jacob, P. Bernhardt, H.G. Paretzke, M. Dingfelder, Radiat. Res. **159**, 401 (2003)
17. A. Lappa, E. Bigildeev, D. Burmistrov, O. Vasilyev, Radiat. Environ. Biophys. **32**, 1 (1993)
18. V. Cobut, L. Cirioni, J. Patau, Nucl. Instrum. Meth. Phys. Res. B: Beam Interactions with Materials and Atoms **215**, 57 (2004)
19. H. Tomita, M. Kai, T. Kusama, A. Ito, Radiat. Environ. Biophys. **36**, 105 (1997)
20. T. Kai, A. Yokoya, M. Ukai, K. Fujii, R. Watanabe, Radiat. Phys. Chem. **115**, 1 (2015)
21. Y. Matsuya, T. Kai, T. Sato, T. Liamsuwan, K. Sasaki, H. Nikjoo, Phys. Med. Biol. **66**, 06NT02 (2021)
22. Y. Hirata, T. Kai, T. Ogawa, Y. Matsuya, T. Sato, Jpn. J. Appl. Phys. **61**, 106004 (2022)
23. Y. Hirata, T. Kai, T. Ogawa, Y. Matsuya, T. Sato, Jpn. J. Appl. Phys. **62**, 106001 (2023)
24. T. Ogawa, Y. Hirata, Y. Matsuya, T. Kai, Sci. Rep. **11**, 24401 (2021)
25. T. Goorley, M. James, T. Booth, F. Brown, J. Bull, L. Cox, J. Durkee, J. Elson, M. Fensin, R. Forster et al., Nucl. Technol. **180**, 298 (2012)
26. S. Agostinelli, J. Allison, K. Amako, J. Apostolakis, H. Araujo, P. Arce, M. Asai, D. Axen, S. Banerjee, G. Barrand et al., Nucl. Instrum. Meth. Phys. Res. A: Accelerators, Spectrometers, Detectors and Associated Equipment **506**, 250 (2003)
27. N.V. Mokhov, Tech. rep. (Fermi National Accelerator Lab., Batavia, IL (US), 2003)
28. G. Battistoni, T. Boehlen, F. Cerutti, P.W. Chin, L.S. Esposito, A. Fassò, A. Ferrari, A. Lechner, A. Empl, A. Mairani et al., *Overview of the FLUKA code*, Vol. 82 (2015), joint International Conference on Supercomputing in Nuclear Applications and Monte Carlo 2013, SNA + MC 2013. Pluri- and Trans-disciplinarity, Towards New Modeling and Numerical Simulation Paradigms, https://www.sciencedirect.com/science/article/pii/S0306454914005878
29. C. Ahdida, D. Bozzato, D. Calzolari, F. Cerutti, N. Charitonidis, A. Cimmino, A. Coronetti, G. D'Alessandro, A. Donadon Servelle, L. Esposito et al., Front. Phys. **9**, 788253 (2022)
30. T. Böhlen, F. Cerutti, M. Chin, A. Fasso, A. Ferrari, P. Ortega, A. Mairani, P. Sala, G. Smirnov, V. Vlachoudis, Nucl. Data Sheets **120**, 211 (2014)
31. A. Ferrari, P.R. Sala, A. Fasso, J. Ranft, *FLUKA: A multi-particle transport code (program version 2005)* (CERN, Geneva, 2005), https://cds.cern.ch/record/898301
32. O. Iwamoto, N. Iwamoto, S. Kunieda, F. Minato, S. Nakayama, Y. Abe, K. Tsubakihara, S. Okumura, C. Ishizuka, T. Yoshida et al., J. Nucl. Sci. Technol. **60**, 1 (2023)
33. H. Iwamoto, S. ichiro Meigo, J. Nucl. Sci. Technol. **56**, 160 (2019)
34. T. Ogawa, S. Hashimoto, T. Sato, K. Niita, Nuclear Instruments and Methods in Physics Research Section B: Beam Interactions with Materials and Atoms **325**, 35 (2014)
35. Y. Sakaki, Y. Namito, T. Sanami, H. Iwase, H. Hirayama, Nucl. Instrum. Meth. Phys. Res. A: Accelerators, Spectrometers, Detectors and Associated Equipment **977**, 164323 (2020)
36. A. Malins, M. Machida, K. Niita, *Continuous energy adjoint transport for photons in PHITS*, in *EPJ Web of Conferences* (EDP Sciences, 2017), Vol. 153, pp. 06001
37. D. Matthiä, T. Berger, A.I. Mrigakshi, G. Reitz, Adv. Space Res. **51**, 329 (2013)
38. A.J. Tylka, W.F. Dietrich, *A new and comprehensive analysis of proton spectra in ground-level enhanced (GLE) solar particle events*, in *31th International Cosmic Ray Conference* (Universal Academy Press Lodź, 2009)
39. T. Sato, A. Nagamatsu, H. Ueno, R. Kataoka, S. Miyake, K. Takeda, K. Niita, Radiat. Prot. Dosimetry **180**, 146 (2018)
40. D.M. Sawyer, J.I. Vette, Tech. rep. (1976)
41. D. Heynderickx, B. Quaghebeur, J. Wera, E. Daly, H. Evans, Space Weather **2**, 10S03 (2004)
42. T. Sato, PloS One **10**, e0144679 (2015)
43. T. Sato, PloS One **11**, e0160390 (2016)
44. K. Nordlund, S.J. Zinkle, A.E. Sand, F. Granberg, R.S. Averback, R.E. Stoller, T. Suzudo, L. Malerba, F. Banhart, W.J. Weber et al., J. Nucl. Mater. **512**, 450 (2018)
45. Y. Iwamoto, S. ichiro Meigo, S. Hashimoto, J. Nucl. Mater. **538**, 152261 (2020)
46. T. Sato, Y. Matsuya, T. Ogawa, T. Kai, Y. Hirata, S. Tsuda, A. Parisi, Phys. Med. Biol. (2023)
47. H.N. Ratliff, N. Matsuda, S. Abe, T. Miura, T. Furuta, Y. Iwamoto, T. Sato, Nucl. Instrum. Meth. Phys. Res. B: Beam Interactions with Materials and Atoms **484**, 29 (2020)
48. D. Satoh, T. Sato, J. Nucl. Sci. Technol. **59**, 1047 (2022)
49. D. Satoh, T. Sato, N. Shigyo, K. Ishibashi, JAEA-Data/Code **23**, 2006 (2006)

50. T. Kai, A. Yokoya, M. Ukai, K. Fujii, M. Higuchi, R. Watanabe, Radiat. Phys. Chem. **102**, 16 (2014)
51. Y. Matsuya, T. Kai, Y. Yoshii, Y. Yachi, S. Naijo, H. Date, T. Sato, J. Appl. Phys. **126**, 124701 (2019)
52. T. Kai, T. Toigawa, Y. Matsuya, Y. Hirata, T. Tezuka, H. Tsuchida, A. Yokoya, RSC Adv. **13**, 7076 (2023)
53. H. Ehrhardt, K. Jung, G. Knoth, P. Schlemmer, Z. Phys. D: At. Mol. Clusters **1**, 3 (1986)
54. R. Ritchie, Phys. Rev. **114**, 644 (1959)
55. T. Liamsuwan, H. Nikjoo, Phys. Med. Biol. **58**, 673 (2013)
56. Y.K. Kim, M.E. Rudd, Phys. Rev. A **50**, 3954 (1994)
57. Y.K. Kim, J.P. Santos, F. Parente, Phys. Rev. A **62**, 052710 (2000)
58. Y.K. Kim, W.R. Johnson, M.E. Rudd, Phys. Rev. A **61**, 034702 (2000)
59. M.J. Berger, M. Inokuti, H.H. Anderson, H. Bichsel, J.A. Dennis, D. Powers, S.M. Seltzer, J.E. Turner, J. Int. Comm. Radiat. Units Measurements **os19**, 55 (2016)
60. M.E. Rudd, Y.K. Kim, D.H. Madison, J.W. Gallagher, Rev. Mod. Phys. **57**, 965 (1985)
61. T. Ogawa, Y. Iwamoto, Nucl. Instrum. Meth. Phys. Res. B: Beam Interactions with Materials and Atoms **549**, 165255 (2024)
62. M.E. Rudd, Phys. Rev. A **38**, 6129 (1988)
63. T. Kanai, Y. Furusawa, K. Fukutsu, H. Itsukaichi, K. Eguchi-Kasai, H. Ohara, Radiat. Res. **147**, 78 (1997)
64. H. Horiguchi, T. Sato, H. Kumada, T. Yamamoto, T. Sakae, J. Radiat. Res. **56**, 382 (2015)
65. A. Parisi, C.J. Beltran, K.M. Furutani, Phys. Med. Biol. **67**, 185013 (2022)
66. T. Sato, S. Hashimoto, T. Inaniwa, K. Takada, H. Kumada, Int. J. Radiat. Biol. **97**, 1450 (2021)
67. T. Sato, Y. Furusawa, Radiat. Res. **178**, 341 (2012)
68. Y. Hirata, T. Sato, K. Watanabe, T. Ogawa, A. Parisi, A. Uritani, J. Nucl. Sci. Technol. **59**, 915 (2022)
69. A. Parisi, O. Van Hoey, P. Mégret, F. Vanhavere, Radiat. Prot. Dosimetry **183**, 72 (2018)
70. T. Ogawa, T. Yamaki, T. Sato, PLOS ONE **13**, 1 (2018)
71. T. Sato, R. Watanabe, K. Niita, Radiat. Prot. Dosimetry **122**, 41 (2006)
72. T. Sato, Y. Kase, R. Watanabe, K. Niita, L. Sihver, Radiat. Res. **171**, 107 (2009)
73. Y. Matsuya, T. Kai, A. Parisi, Y. Yoshii, T. Sato, Phys. Med. Biol. **67**, 215017 (2022)
74. Y. Matsuya, T. Nakano, T. Kai, N. Shikazono, K. Akamatsu, Y. Yoshii, T. Sato, Int. J. Mol. Sci. **21**, 1701 (2020)
75. Yusuke Matsuya, Takeshi Kai, Tatsuhiko Sato, Tatsuhiko Ogawa, Yuho Hirata, Yuji Yoshii, Alessio Parisi, Thiansin Liamsuwan, Int. J. Radiat. Biol. **98**, 148 (2022), pMID: 34930091
76. Y. Matsuya, Y. Yoshii, T. Kusumoto, K. Akamatsu, Y. Hirata, T. Sato, T. Kai, Phys. Med. Biol. (2023)
77. F.D. Becchetti, C. Thorn, M. Levine, Nucl. Instrum. Meth. **138**, 93 (1976)
78. G. Kinchin, R. Pease, Rep. Progr. Phys. **18**, 1 (1955)
79. Y. Iwamoto, Nucl. Instrum. Meth. Phys. Res. B: Beam Interactions with Materials and Atoms **419**, 32 (2018)
80. J.F. Ziegler, M. Ziegler, J. Biersack, Nucl. Instrum. Meth. Phys. Res. B: Beam Interactions with Materials and Atoms **268**, 1818 (2010), 19th International Conference on Ion Beam Analysis
81. K. Niita, Y. Iwamoto, T. Sato, H. Iwase, N. Matsuda, Y. Sakamoto, H. Nakashima, A new treatment of radiation behaviour beyond one-body observables, in *International Conference on Nuclear Data for Science and Technology* (EDP Sciences, 2007), pp. 1167–1169
82. T. Ogawa, T. Sato, S. Hashimoto, K. Niita, Nucl. Instrum. Meth. Phys. Res. A: Accelerators, Spectrometers, Detectors and Associated Equipment **763**, 575 (2014)
83. S. Noda, S. Hashimoto, T. Sato, T. Fukahori, S. Chiba, K. Niita, J. Nucl. Sci. Technol. **52**, 57 (2015)

Cite this article as: Tatsuhiko Ogawa, Yuho Hirata, Yusuke Matsuya, Takeshi Kai, Tatsuhiko Sato, Yosuke Iwamoto, Shintaro Hashimoto, Takuya Furuta, Shin-ichiro Abe, Norihiro Matsuda, Takuya Sekikawa, Lan Yao, Pi-En Tsai, Hunter N. Ratliff, Hiroshi Iwase, Yasuhito Sakaki, Kenta Sugihara, Nobuhiro Shigyo, Lembit Sihver, Koji Niita. Overview of PHITS Ver.3.34 with particular focus on track-structure calculation, EPJ Nuclear Sci. Technol. **10**, 13 (2024)